Correlation functions, free energies, and magnetizations in the two-dimensional random-field Ising model

S. L. A. de Queiroz[1,*] and R. B. Stinchcombe[2,†]
[1]*Instituto de Física, Universidade Federal do Rio de Janeiro, Caixa Postal 68528, 21945-970 Rio de Janeiro RJ, Brazil*
[2]*Department of Physics, Theoretical Physics, University of Oxford, 1 Keble Road, Oxford OX1 3NP, United Kingdom*
(Received 16 May 2001; published 28 August 2001)

Transfer-matrix methods are used to calculate spin-spin correlation functions (G), Helmholtz free energies (f) and magnetizations (m) in the two-dimensional random-field Ising model close to the zero-field bulk critical temperature $T_{c\ 0}$, on long strips of width $L=3-18$ sites, for binary field distributions. Analysis of the probability distributions of G for varying spin-spin distances R shows that describing the decay of their averaged values by effective correlation lengths is a valid procedure only for not very large R. Connections between field and correlation function distributions at high temperatures are established, yielding approximate analytical expressions for the latter, which are used for computation of the corresponding structure factor. It is shown that, for fixed R/L, the fractional widths of correlation-function distributions saturate asymptotically with $L^{-2.2}$. Considering an added uniform applied field h, a connection between $f(h)$, $m(h)$, the Gibbs free energy $g(m)$ and the distribution function for the uniform magnetization in a zero uniform field, $P_0(m)$, is derived and first illustrated for pure systems, and then applied for nonzero random field. From finite-size scaling and crossover arguments, coupled with numerical data, it is found that the width of $P_0(m)$ varies against (nonvanishing, but small) random-field intensity H_0 as $H_0^{-3/7}$.

DOI: 10.1103/PhysRevE.64.036117 PACS number(s): 05.50.+q, 75.10.Nr, 64.60.Fr

I. INTRODUCTION

The random-field Ising model (RFIM) has posed a number of challenges to researchers since its introduction as an apparently purely theoretical puzzle [1]. The later realization that it corresponds, give or take a few (hopefully irrelevant) details, to the experimentally realizable dilute Ising antiferromagnet in a uniform applied field [2] brought about new insights and new questions as well; among the latter, is the interpretation of experimental data in a suitable theoretical framework. This has proved to be rather an intricate subject, even down to basic aspects such as whether the lower critical dimensionality for the problem was $d=2$ or 3 [3–5]. Though by now this particular issue was settled in favor of $d=2$ [6], several important aspects (such as the scaling behavior near the destroyed phase transition in $d=2$, which will be of interest here) still require further elucidation [7].

In the present paper we deal with a two-dimensional RFIM, where long-range order is destroyed, and a zero-temperature, zero-field ''anomalous'' critical point appears [8]. The latter will not concern us directly, as we shall be working at high temperatures, close to the pure-system ferroparamagnetic transition. We extend and complement our early work [9], making use of transfer-matrix (TM) methods on long, finite-width strips of a square lattice; we generate and analyze statistics of spin-spin correlation functions and uniform magnetizations. Wherever feasible, we attempt to draw connections between our numerical results and experimentally observable quantities. In what follows, we begin by briefly reviewing selected aspects of the numerical techniques used, and how they relate to the physical problem under study. We then recall the connection between structure factors and averaged correlations in random systems, and discuss the extraction of effective correlation lengths from our numerical data for correlation-function statistics. Next we exploit the connection between field and correlation function distributions at high temperatures, in an attempt to derive approximate analytical expressions for the latter; such formulas are used in turn, in order to compute the corresponding structure factor. A short section is dedicated to a reanalysis of the asymptotic behavior of the widths of correlation function distributions, first presented in Ref. [9], and now complemented by additional data. In Sec. VI, an additional uniform applied field is considered: free energies and uniform magnetizations are calculated on strips of both pure and RFIM systems. These quantities are used to calculate the corresponding Gibbs free energy which, in turn, gives the distribution function for the uniform magnetization in zero uniform field. Numerical data are then analyzed via finite-size scaling and crossover arguments. A final section summarizes our work.

II. NUMERICAL METHODS AND $d=2$ RFIM

We consider strips of a square lattice of ferromagnetic Ising spins with nearest-neighbor interaction $J=1$, of width $3\leqslant L\leqslant 18$ sites with periodic boundary conditions across. The random-field values h_i are drawn for each site i from the binary distribution:

$$p(h_i)=\tfrac{1}{2}[\,\delta(h_i-H_0)+\delta(h_i+H_0)\,]. \tag{1}$$

TM methods are used, on long strips of typical length $L_x=10^6$ columns, as described at length in Ref. [9] and references therein, to generate representative samples of the quenched random fields. Along the strip, we calculate corre-

*Electronic address: sldq@if.ufrj.br
†Electronic address: stinch@thphys.ox.ac.uk

lation functions (as explained in the next paragraph), as well as free energies and magnetizations (details in Sec. VI).

Here we calculate the disconnected spin-spin correlation function $G(R) \equiv \langle \sigma_0^1 \sigma_R^1 \rangle$, between spins on the same row (say, row 1), and R columns apart. Related quantities, such as correlation lengths, are defined with connected correlations, $\langle \sigma_0 \sigma_R \rangle - \langle \sigma \rangle^2$, in mind; however, for the quasi-one-dimensional Ising systems under consideration (either pure or random) one is always in the paramagnetic phase, so the distinction between connected and disconnected correlations is unimportant. In Ref. [9] we explained why the ranges of spin-spin distance, temperature, and random-field intensity of most interest for investigation by TM methods are, respectively, $R/L \simeq 1$, $0 < T \lesssim T_{c\ 0} = 2.269\ldots$ [we take $k_B \equiv 1$], $H_0 \lesssim 0.5$. Here we restrict ourselves to high temperatures $T \gtrsim 2.0$ and rather low fields $H_0 \lesssim 0.1 - 0.15$. We use a linear binning for the histograms of occurrence of $G(R)$; usually the whole $[-1,1]$ interval of variation of $G(R)$ is divided into 10^3 bins.

Since we shall be dealing with probability distributions, a word is in order about multifractality. Though multifractal behavior has been found *at* the critical point of random-bond Potts systems [10,11], the available evidence strongly suggests that, off bulk criticality, correlation functions behave normally [10]. Thus in the present case we expect that analyses of different moments of the probability distribution of G will yield essentially the same results.

III. CORRELATION DECAY

The properties of correlation functions are usually incorporated into associated correlation lengths, whose basic definition is as (minus) the inverse slope of semilogarithmic plots of correlation functions against distance. In this view, one assumes both that exponential decay can be well defined at essentially all distances, and that a single length is enough to characterize such behavior. In cases such as the present, quenched randomness implies that configurational averages must be taken, and one must be careful in deciding what quantities are to be thus promediated. Recall that, e.g., in neutron scattering experiments, the intensity of the magnetic critical scattering is proportional to the average (over the crystal) of the scattering function $S(\vec{q})$, which is the Fourier transform of the correlation function for wave-vector transfer $\vec{q}$ [12,13]. With $G_R \equiv G(R)$, and wave vector q in the row direction S becomes

$$[S(q)] = \left[\int dR\, e^{iqR} G_R \right] = \int dR\, e^{iqR} \langle G_R \rangle, \qquad (2)$$

where $[\cdots]$ stands for configurational average, and

$$\langle G_R \rangle = \int dG_R\, P(G_R) G_R, \qquad (3)$$

where $P(G_R)$ is the probability distribution for G_R. The last equality in Eq (2) depends only on the assumption that $P(G_R)$ is position independent along the crystal.

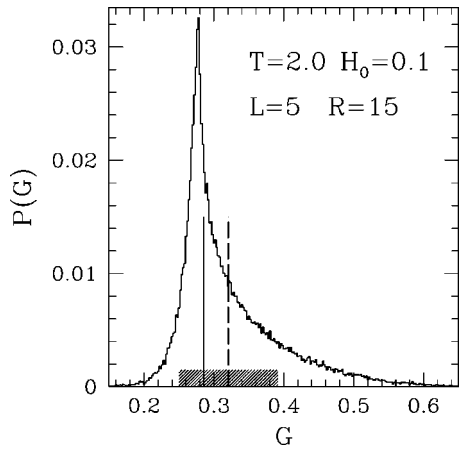

FIG. 1. Normalized histogram $P(G)$ of the occurrence of G. Strip length $L_x = 10^6$ columns, binwidth 2×10^{-3}. Vertical bars are located at G_0 (full line) and $\langle G \rangle$ (dashed), respectively. The shaded region on the horizontal axis goes from $\langle G \rangle - \tilde{W}$ to $\langle G \rangle + \tilde{W}$.

The simplest assumption for $P(G_R)$ that incorporates both disorder and exponential decay given by a single length ξ for all distances is a Gaussian distribution

$$P(G_R) = \frac{1}{\sqrt{2\pi}\,\Delta(R)} e^{-y^2/2\Delta^2(R)}, \quad y \equiv G_R - e^{-R/\xi}, \quad (4)$$

where distance-dependent widths $\Delta(R)$ allow for, e.g. (disorder-induced), larger uncertainties for larger spin-spin separations. However, using Eq. (4) in Eqs. (2) and (3), one obtains a width-independent Lorentzian form for the average structure factor:

$$[S(q)] = \frac{1}{q^2 + \dfrac{1}{\xi^2}}. \qquad (5)$$

This coincides with the standard mean-field result for the disordered phase, and is deemed unsatisfactory upon comparison with experimental data [7,13].

We now exhibit our numerical results, and compare their implications to those of Eqs. (4) and (5). For high temperatures and low random-field intensities, as specified above, we recall (also see Ref. [9]) the following main features found for the probability distribution $P(G)$: (i) a clearly identifiable, cusplike peak, at some G_m *below* the zero-field value $G_0 \equiv G(H_0 = 0)$; (ii) a short tail below the peak and a long one above it, such that (iii) all moments of order $\geqslant 0$ of the distribution are *above* G_0. In Fig. 1, where the first moment $\langle G \rangle$ is shown, one has $G_m = 0.278$, $G_0 = 0.2853$, $\langle G \rangle = 0.321$; the rms width $\tilde{W} \equiv \langle (G - \langle G \rangle)^2 \rangle^{1/2} = 0.071$.

Therefore, the features depicted in Fig. 1, especially the asymmetric cusp, are at variance with the form of Eq. (4). We now investigate what effects are carried over to the associated correlation lengths. We do so by mimicking the procedure outlined in Eqs. (2) and (3) above: first we average over randomness for a given spin-spin separation, and then study the variation of the averaged quantities over distance.

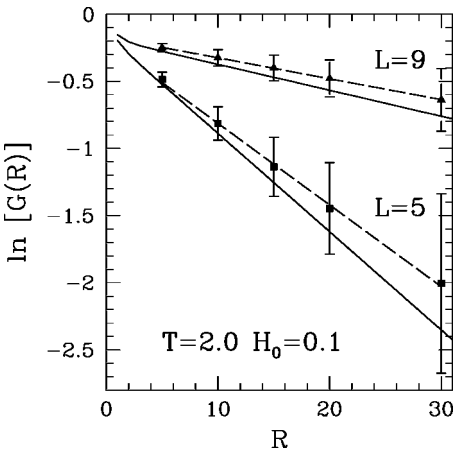

FIG. 2. Correlation decay along strips of widths $L=5$ and 9. Full lines: $H_0=0$. Points: $\langle G\rangle$ for $H_0=0.1$. Dashed lines: unweighted least-squares fits of $H_0=0.1$ data. Vertical bars give the rms widths $\tilde{W}$ of corresponding distributions.

The results are in Fig. 2, where our numerical data for $\langle G\rangle$ are plotted against varying R. $H_0=0$ data are also shown for comparison.

One sees from the respective slopes that, taking into account data for $R\gtrsim L$, the correlation length for $H_0\neq 0$ would seem to be systematically *larger* than in zero field. This reflects the domain structure into which the system breaks down: at short distances the conditional probability for a spin to belong to the same domain as the one at the origin is *larger* than for $H_0=0$.

For longer distances, correlation functions start to show severe disorder-induced fluctuations, related to the crossing of domain walls. Contrary to the zero-field case, where temperature-induced domain walls are present but the respective sign changes in correlation functions average out to give an exponential fall off, here the domain wall configurations are essentially determined by the (quenched) accumulated random-field fluctuations. At large R, such fluctuations play a very sensitive role even for very low random field intensities. One anticipates problems with defining correlation lengths from the corresponding data. The vertical bars in Fig. 2 show that, for a fixed strip width L, the width $\tilde{W}$ of the distribution indeed grows apparently unbounded for increasing R; though this is related to the crossing of domain walls just mentioned, it is also, and predominantly, an intrinsic feature of the quasi-one-dimensional systems used here. Thus inferring a two-dimensional behavior from such trends may be risky. However, we now argue that in $d=2$ one does actually run into problems for large R, exactly as inferred above; only, the underlying reasoning is subtler.

In fact (see Ref. [9] and Sec. V below), a different analysis of correlation functions, at fixed R/L, strongly suggests that the *relative* widths $W\equiv\tilde{W}/\langle G\rangle$ grow as $R,L\to\infty$ in $d=2$, approaching a finite limiting value $C H_0^{\kappa}$, $C\simeq 2$, $\kappa\simeq 0.5$. This means that, when one considers the dispersion of $\ln\langle G\rangle$, the signal-to-noise ratio becomes of order 1 for large R,L, and it is this latter fact that, in $d=2$, must compromise attempts to extract correlation lengths in such range.

The effect of the above on fits of neutron-scattering data to line shapes is that, since the latter rely on the idea that correlation lengths are always reliable quantities, they may be off the actual picture in the small-wavevector region. We now attempt to derive approximate analytical expressions for $P(G_R)$; our ultimate goal is to predict a form for $[S(q)]$ from Eqs. (2) and (3).

IV. DISTRIBUTION OF G FROM FIELD DISTRIBUTION (AT HIGH T)

In this section we use simple scaling ideas to establish a quantitative connection between the underlying distribution of accumulated fields and that of the correlation functions themselves. We begin by considering a one-dimensional system with sites denoted by $i=0,1,\ldots,$ uniform nearest-neighbor interactions K and site-dependent random fields h_i (both in units of T). For any given specific realisation of the fields an exact decimation scheme with length scaling factor $b=2$ can be applied, eliminating all odd-numbered sites. The renormalized fields at, and coupling between, e.g., spins 0 and 2, are given by

$$h_0'-h_2'=h_0-h_2,$$

$$h_0'+h_2'=h_0+h_2+\frac{1}{2}\ln\left[\frac{\cosh 2(K+h_1)}{\cosh 2(K-h_1)}\right], \tag{6}$$

$$4K'=\ln\left[\frac{\cosh 2(K+h_1)\cosh 2(K-h_1)}{\cosh^2 2h_1}\right].$$

Iterating this procedure n times, one obtains a single renormalized bond $\tilde{K}$ connecting sites 0 and R ($R=2^n$), at which the respective rescaled fields are $\tilde{h}_0$, $\tilde{h}_R$. The correlation function $G(R)\equiv\langle\sigma_0\sigma_R\rangle$ is therefore

$$G(R)=\frac{e^{2\tilde{K}}\cosh(\tilde{h}_0+\tilde{h}_R)-\cosh(\tilde{h}_0-\tilde{h}_R)}{e^{2\tilde{K}}\cosh(\tilde{h}_0+\tilde{h}_R)+\cosh(\tilde{h}_0-\tilde{h}_R)}. \tag{7}$$

For low fields $H_0\ll 1$, one uses $\cosh(\tilde{h}_0-\tilde{h}_R)/\cosh(\tilde{h}_0+\tilde{h}_R)\simeq\exp(-2\tilde{h}_0\tilde{h}_R)$ to obtain

$$G(R)\simeq\tanh(\tilde{K}+\tilde{h}_0\tilde{h}_R). \tag{8}$$

Then, also provided that $H_0\ll K$, the distribution of $G(R)$ is given by that of $X\equiv\tilde{h}_0\tilde{h}_R$, since (to lowest order in H_0) $K'=\frac{1}{2}\ln\cosh 2K$ is field independent. One has

$$P(X)=\int d\tilde{h}_0\,\tilde{P}(\tilde{h}_0)\int d\tilde{h}_R\,\tilde{P}(\tilde{h}_R)\,\delta(X-\tilde{h}_0\tilde{h}_R). \tag{9}$$

At low H_0, the scaling equations (6) give $h_0'\sim h_0+h_1\tanh 2K$. Repeated applications of this transformation give $\tilde{h}_0\sim\Sigma_{i=1}^{R}h_i$ if $R\ll\xi$, where $\xi\sim\ln(\tanh K)^{-1}$ is the correlation length at low H_0. Then $\tilde{h}_0$ (and similarly $\tilde{h}_R$) is the

sum of $\mathcal{N}$ independent variables ($\mathcal{N}=R$), so the individual distributions of $\tilde{h}_0$, $\tilde{h}_R$ become (at large R and ξ) Gaussians of width $\Delta \equiv H_0\sqrt{\mathcal{N}}$:

$$\tilde{P}(\tilde{h}_{0,R}) \propto \exp[-(\tilde{h}_{0,R}/\Delta)^2]. \tag{10}$$

For $R \gtrsim \xi$, the same form applies, but because the field accumulation under scaling is cut off by the decreasing $\tanh K$, the relation for Δ involves $\mathcal{N} \sim \xi$. So, in general, $\mathcal{N} \sim \min(R,\xi)$.

Making $\tilde{h}_0 = s\cos\theta$, $\tilde{h}_R = s\sin\theta$,

$$P(X) \propto \int_0^\infty ds\, s \int_0^{2\pi} d\theta\, e^{-s^2/\Delta^2}\, \delta\left(X - \frac{s^2}{2}\sin 2\theta\right), \tag{11}$$

with the final result

$$P(X) = \frac{a}{\Delta^2} e^{-y} \ln\left(1+\frac{1}{y}\right), \quad y \equiv \frac{2|X|}{\Delta^2}, \tag{12}$$

where a is an overall normalization constant. Strictly speaking, Eq. (12) is an *asymptotic* reduction of Eq. (11), valid for the regimes $y \ll 1$ (the relevant one for our purposes, as shown below) and $y \gg 1$.

Transforming back to $P(G)$, one sees that the value G_m for which $P(G)$ is maximum must correspond to $X=0$, which maximizes $P(X)$. Thus, from Eq. (8),

$$y = \frac{2}{\Delta^2}|\tanh^{-1} G_m - \tanh^{-1} G|. \tag{13}$$

For G close to G_m, linearization gives

$$P(G) \sim \frac{\exp\left[-\frac{1}{\tilde{\Delta}^2}|G_m - G|\right]}{2\Delta^2[1-G^2]} \ln\left[1+\frac{\tilde{\Delta}^2}{|G_m - G|}\right], \tag{14}$$

with $\tilde{\Delta}^2 = \frac{1}{2}\Delta^2(1-G_m^2)$.

The main feature exhibited by this form is a locally symmetric cusp, with infinite slope on either side, at $G=G_m$. This is expected to carry over to more general contexts, provided that $H_0 \ll 1$. Indeed we have checked that a similar description (applying approximate Migdal-Kadanoff scaling calculations), with the prediction of a cusp, also applies on strips and in two dimensions [see Eqs. (15) and (16) below, and related discussion]. A quantitative test of Eq. (14) is shown in Fig. 3, where only data for $G \leqslant G_m$ are displayed (we shall deal with $G > G_m$ immediately afterward). The conditions are such that $R \lesssim \xi$, $G_m^2 \ll 1$ (see Fig. 2), so the above low-field theory gives $\tilde{\Delta} \sim H_0\sqrt{R}$. One sees that exponential decay against $|G-G_m|/RH_0^2$ is indeed the dominant behavior, provided that $H_0 \lesssim 0.15$; already for $H_0 = 0.25$, small departures show, which become more prominent for $H_0 = 0.5$.

As regards cusp asymmetry, not predicted by Eq. (14), we have found that although data for $G > G_m$ still fall exponentially for small H_0, they do not collapse when plotted against

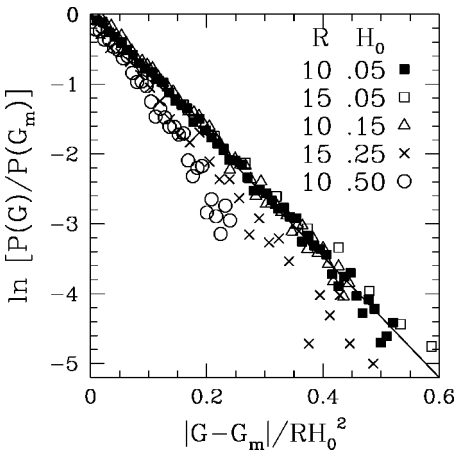

FIG. 3. Semilogarithmic plots of distribution functions below G_m, the value at which $P(G)$ peaks (see text). $L=5$ and $T=2.0$. The straight line is a guide to the eye.

$|G-G_m|/RH_0^2$. This is because the mutual reinforcement, between ferromagnetic spin-spin interactions and accumulated field fluctuations (responsible for the long forward tail [9]), is left out by the approximation above Eq. (9), namely, that K' is H_0 independent.

Before calculating $[S(q)]$ from Eq. (14), we recall that Eqs. (2) and (3) are normally required for bulk systems, thus one must work out an approximate scheme to go from the $d=1$ regime of Eqs. (6)–(14) to $d=2$. We have done so via a Midgal-Kadanoff rescaling transformation at $T \sim T_{c\,0}$. As a consequence of the similarity of the corresponding recursion relations, to those for one dimension, one ends up, after m scalings such that $2^m = R$, with a result very similar to Eq. (8),

$$G(R) = \tanh(\tilde{K} + \tilde{h}_0\tilde{h}_R), \tag{15}$$

where again one assumes low fields, $\tilde{h}_0$, $\tilde{h}_R$. For large R these have Gaussian distributions of width Δ_R determined by the eigenvalue λ of the low-field scaling transformation of H_0. For T near $T_{c\,0}$, $\Delta_R \propto R^\mu H_0$ where $\mu = \ln\lambda/\ln b$ ($b=2$). Further,

$$\tilde{K} \sim K_c - \frac{R}{\xi}. \tag{16}$$

Since Eqs. (9)–(12) still apply, provided Δ is replaced by Δ_R, one obtains the dominant contribution to the scattering function as:

$$[S(q)] \propto \mathrm{Re}\int dR\, e^{iqR} e^{-R/\xi}(1 + C\,\Delta_R^2), \tag{17}$$

where C is a constant of order unity. This can be transformed into

$$[S(q)] \propto \frac{1/\xi}{\frac{1}{\xi^2}+q^2} + CH_0^2(2\mu)!\,\mathrm{Re}\left(\frac{1}{\xi} - iq\right)^{-(2\mu+1)}. \tag{18}$$

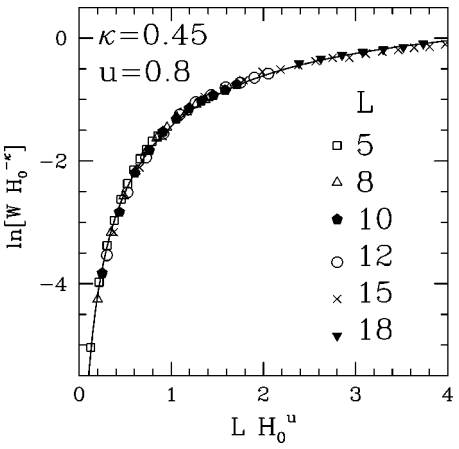

FIG. 4. Semilogarithmic scaling plot of rms relative widths $W H_0^{\kappa}$ against $L H_0^u$. The curve is a fitting spline given by Eq. (20).

If one assumes the form $\Delta = H_0 \sqrt{R}$, given for $R \leqslant \xi$ in one dimension [see above and below Eq. (10)], and also by the Migdal-Kadanoff scheme in $d=2$, then $\mu = 1/2$, and Eq. (18) predicts the line shape to be Lorentzian plus Lorentzian-squared, the mean-field form found when the disconnected contribution is taken into account [4,7,12–14]. On the other hand, if ones goes by the saturation behavior predicted in Ref. [9] and in Sec. V below, and by the scaling approaches if $R \gtrsim \xi$, then the result is $\zeta = 0$, corresponding to a single Lorentzian in Eq. (18).

Though either of these final predictions is certainly open to challenge, in view of the number and severity of approximations involved in the course of their derivation, it is expected that the procedure described above will serve as a rough guide to attempts at connecting basic microscopic features (such as fluctuations of accumulated fields) to observable quantities, e.g., scattering functions.

V. WIDTHS OF *G* DISTRIBUTION

In Ref. [9] we studied the variation of the rms relative width W of the probability distribution of correlation functions, against the field intensity and strip width, for fixed R/L, high temperatures and small H_0. We proposed the scaling form

$$W = H_0^{\kappa} f(L H_0^u), \tag{19}$$

and showed that, for $R/L=1$, $T=T_{c\ 0}$, good data collapse of $y \equiv \ln[W H_0^{-\kappa}]$ against $x \equiv L H_0^u$ can indeed be obtained with $\kappa \simeq 0.43-0.50$ and $u \simeq 0.8$. We used $L \leqslant 15$ and scanned $0 < x \lesssim 2.8$; keeping $\kappa = 0.45$ and $u = 0.8$, we found for $x > 1$ a satisfactory fit given by $y = -0.3 - 5.3 \exp(-1.57x)$, which would imply an exponential saturation of the scaled width $W h_0^{-\kappa}$ as $x \to \infty$, with a limiting value $\exp(-0.3) = 0.83$.

In Fig. 4, we display again the data of Ref. [9], plus additional data for $L=15$ and 18, which enabled us to explore larger values of x ($x \lesssim 4.0$) while still keeping to relatively low H_0. We then reanalyzed our full set of data, with the results that (i) we managed an excellent fit to the whole interval $0 < x < 4$ by a single expression

$$y = -2.2 \left\{ \ln\left(\frac{1.0}{x} + 0.6 \right) \right\} - 0.4025, \tag{20}$$

(in which y and x involve the same values of the exponents κ, u as earlier), and (ii) this new fit, while still predicting saturation for $x \gg 1$, implies that in the approach to two dimensions $x \gg 1$, convergence of $W h_0^{-\kappa}$ is power law like, giving a limiting scaled width $W h_0^{-\kappa} = 0.6^{-2.2} \exp(-0.4025) = 2.06$.

VI. MAGNETIZATIONS

In this section we examine the scaling properties of the uniform magnetization on strips of the $d=2$ RFIM. For convenience we shall always keep $T = T_{c\ 0}$.

We first outline our method, which involves a generalized Legendre transformation. Consider the Hamiltonian

$$\mathcal{H} = \mathcal{H}_0(\{\sigma\}) - h \sum_i \sigma_i \tag{21}$$

where σ_i are Ising spins, and $\mathcal{H}_0$ includes all interactions except that of the spins with the uniform field h. One has, for the corresponding partition function $Z(h)$,

$$\frac{Z(h)}{Z(0)} = \sum_M P_0(M) e^{\beta M h}, \quad \beta = \frac{1}{T}, \tag{22}$$

where $P_0(M)$ is the probability of occurrence of the value M for the magnetization, *in zero uniform field*. Assuming a system with $N \gg 1$ spins, with $f(h)$ equivalent to the negative free energy per site in units of T, and $m \equiv \beta M/N$,

$$e^{N(f(h)-f(0))} = N \int dm\, P_0(m) e^{N m h}. \tag{23}$$

In order for extensivity to be satisfied, one must have $N P_0(m) = \exp N g(m)$, where $g(m)$ is intensive and determined by

$$e^{N(f(h)-f(0))} = \int dm\, e^{N[g(m) + m h]}. \tag{24}$$

Assuming the usual sharp-peaked distribution around a thermodynamically averaged value $\overline{m}$, one sees that

$$f(h) - f(0) = g(\overline{m}) + \overline{m} h + O\left(\frac{\ln N}{N} \right), \tag{25}$$

with $(dg/dm)_{\overline{m}} = -h$. That is, g is the standard Gibbs free energy per site. Substituting back in Eq. (23), one obtains:

$$P_0(M) = \exp N g(m), \tag{26}$$

where terms of $O(\ln N/N)$ have again been neglected.

Equation (26), with $g(m)$ given through Eq. (25), is the natural starting point to study magnetization distributions by TM methods. Indeed, though one can obtain the thermodynamically averaged exact values of all *moments* of the distribution via the TM method [15,16], the distribution itself is

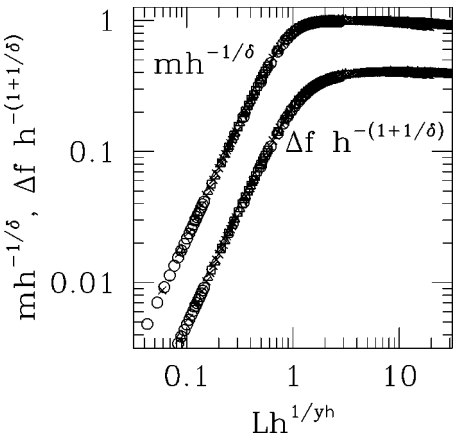

FIG. 5. Scaling plots of magnetization and excess free energy for pure Ising systems at criticality. Strip widths $L=4$ (circles), 8 (crosses), 12 (triangles), and 16 (squares). Normalized magnetizations ($=T_c\,\partial f/\partial h$) are used to avoid a superposition of plots.

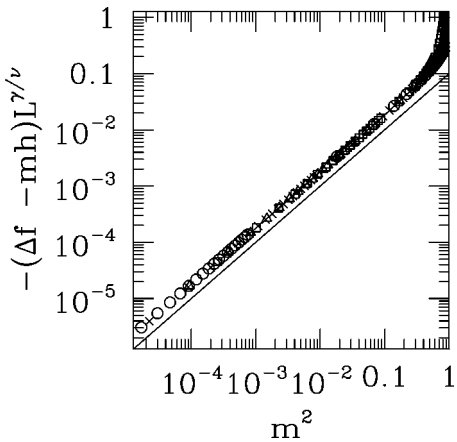

FIG. 6. Negative Gibbs free energy $-g=-(\Delta f-mh)$ times $L^{\gamma/\nu}$ against m^2 for pure Ising systems at criticality. For a key to the symbols, see the caption of Fig. 5. The straight line has a unitary slope, and is a guide to the eye. Normalized magnetizations on the horizontal axis only.

not given directly. This contrasts with Monte Carlo methods, which inherently incorporate readily observable fluctuations around equilibrium, and have been widely used to study magnetization distributions at criticality, both in hypercubic geometries [17] and on planar lattices with various aspect ratios [18].

Recall that, on strips of width L and length L_x, $L_x \gg L$ such as is the case here, the aspect ratio is essentially infinite, therefore $P_0(M)$ will be Gaussian, at least for pure systems [16,18]. Our purpose (as shown below) is to compare pure—and RFIM— results and explain their mutual differences, by using general theory of RF systems [2,8,19–21] coupled with finite-size scaling (FSS) [22].

A. Pure Ising systems

We start by illustrating the properties of $g(m)$ for pure Ising spins. One calculates $f(h)$, $f(0)$, $m(h)$ in Eq. (25) by standard numerical methods [23]: the first two by isolating the largest eigenvalue Λ_0 of the TM and using $f=L^{-1}\ln\Lambda_0$ (which is tantamount to assuming $L_x\to\infty$; more on this below), the third by calculating derivatives of f relative to h. The latter is done here by perturbation theory [15,16,24,25], both for better numerical accuracy and because an adapted procedure proves convenient when dealing with the RF case, where samples over disorder must be accumulated.

At $t\equiv(T-T_c)/T_c=0$, for the excess free energy FSS [22] gives $\Delta f(h,L)\equiv f(t=0,h,L)-f(0,0,L)=h^{1+1/\delta}F(L\,h^{1/y_h})$, with $\delta=15$, $y_h=15/8$. In Fig. 5 we show scaling plots of $\Delta f(h)\,h^{-(1+1/\delta)}$ and $m\,h^{-1/\delta}$ against $L\,h^{1/y_h}$. For low fields ($h\lesssim L^{-y_h}$), the slopes of both logarithmic plots are given by the (finite-size) initial susceptibility exponent $\gamma/\nu=7/4$, as a consequence of the scaling relation $y_h(1-1/\delta)=\gamma/\nu$.

For nonzero t but still for low fields, one generally expects $\Delta f(h)=a(t,L)\,h^{\mu}$ from which $m=a(t,L)\,\mu\,h^{\mu-1}$, $g=\Delta f-mh=a(t,L)\,(1-\mu)\,h^{\mu}$, implying $g\sim a(t,L)^{-1/(\mu-1)}m^{\mu/(\mu-1)}$. Subcases are (i) $t=0$, $L=\infty$: $\Delta f\sim h^{1+1/\delta}$, so $g\sim m^{1+\delta}$; (ii) t small, $L=\infty$, $1\gg t\gtrsim m^{1/\beta}$: $\Delta f=a(t)\,h^2$, $a(t)=\frac{1}{2}\chi(t)\sim t^{-\gamma}$, so $g\sim t^{\gamma}m^2$; and (iii) $t=0$, L finite, $1\ll L\lesssim m^{-\nu/\beta}$: $\Delta f=a(L)\,h^2$, $a(L)=\frac{1}{2}\chi(L)\sim L^{\gamma/\nu}$, so $g\sim L^{-\gamma/\nu}m^2$.

Case (iii) is depicted in Fig. 6. One sees that $-g\,L^{\gamma/\nu}\sim m^2$ as far as $m\simeq 0.6$, which [through Eq. (26)] is consistent with the Gaussian behavior predicted for $P_0(M)$ in this case. Close to $m=1$ scaling breaks down, and the deviation from saturation magnetization must follow a single-spin-flip picture, $\varepsilon\equiv 1-m\sim\exp(-2/T_c)$. The effects of this on g can be worked out from a high-field expansion, in which $\mathcal{H}_0$ of Eq. (21) is taken as a perturbation on the field term $h\Sigma_i\sigma_i$ [26]. The result is

$$\frac{dg}{d\varepsilon}=s_0+\frac{1}{2}\ln\frac{1}{\varepsilon}+O(\varepsilon), \tag{27}$$

where $s_0=\frac{1}{2}(\ln 2-8/T_c)=-1.41617\ldots$.

Figure 7 shows that Eq. (27) is in excellent agreement with numerics already for $(1/2)\ln(1/\varepsilon)\simeq 2.4(\varepsilon\simeq 10^{-2})$. This provides a rigorous check of our analytical and numerical procedures.

Returning to the connection between g and magnetization distributions, we first note that, although we are using $f=L^{-1}\ln\Lambda_0$ which holds only for strip length $L_x\to\infty$, the number $N=L_xL$ of spins in Eq. (26) implies a finite, though possibly very long, strip for the equation to be of practical use. An estimate of the error implied by using infinite-strip free energies instead of their fully-finite system counterparts can be obtained by referring to Table 2 of Ref. [16], where it is shown that for systems with aspect ratio $\alpha\equiv L_x/L=100$, the corresponding value of the Binder parameter $Q\equiv\langle M^2\rangle^2/\langle M^4\rangle$ is $\simeq 2\%$ off its $\alpha\to\infty$ limit of 1/3. As typical widths used here and, especially in Sec. VI B, are in the range $L\lesssim 20$, and assuming that errors in the distribution and in its calculated moments are of the same order, it follows that using the infinite-strip expression for f implies deviations in $P_0(M)$ smaller than 2% for $L_x\gtrsim 2000$. The advantage of this procedure is that L_x can be seen essentially as a

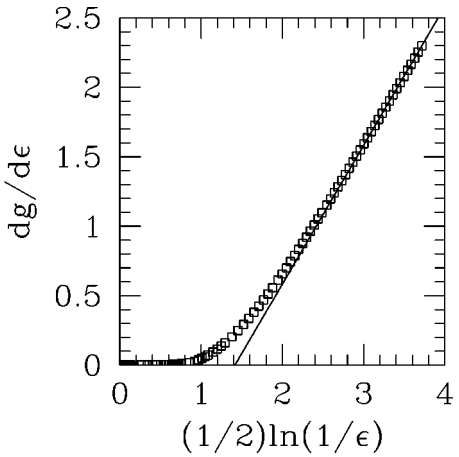

FIG. 7. Derivative of Gibbs free energy relative to the magnetization deviation ε against $(1/2)\ln(1/\varepsilon)$. Points: numerically calculated derivatives from $L=16$ data for f and m ($L=8$ already gives results indistinguishable from those displayed). Straight line: first two terms on the right hand side of Eq. (27).

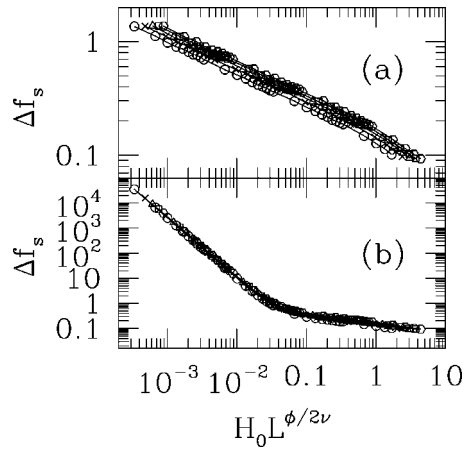

FIG. 8. $\Delta f_s \equiv (\Delta' f(L,H_0) - \tilde{A} L^{-2} \ln H_0) H_0^{-2d\nu/\phi}$ plotted against $H_0 L^{\phi/2\nu}$, $\phi=7/4$, and $\nu=1$. (a) $\tilde{A}=0$. Bottom to top: $L=4$, 6, 8, 10, and 12. (b) $\tilde{A}=10^{-4}$, same notation.

free parameter, i.e., not connected to an actual number of iterations along the strip. For our purposes here, we shall always be comparing pure-system results (where L_x is fictitious in the sense just described) with those obtained on RF strips of the same width at the same temperature, where sampling over disorder typically necessitates an actual $L_x \simeq 10^5$; thus equating the values of L_x in both systems is both correct as far as comparisons are concerned and, given the lengths required for adequate sampling over randomness, fully within acceptable error margins for the description of pure systems.

From Eq. (26), for case (iii) where $-g\,L^{\gamma/\nu} \sim g_0\, m^2$, $g_0 \simeq 10^{-1}$ as shown in Fig. 6,

$$P_0(M) = \exp[-g_0 L_x L^{(\eta-1)} m^2], \tag{28}$$

where $2-\eta=\gamma/\nu$ was used. Therefore, the width of the Gaussian distribution is $\mathcal{W} \sim g_0^{-1/2} L^{(1-\eta)/2}/\sqrt{L_x}$.

B. RFIM

We now include the term $\Sigma_i h_i \sigma_i$ in $\mathcal{H}_0$ of Eq. (21), with the local fields h_i distributed according to Eq. (1). We first consider the application of FSS to the RFIM in a zero uniform field. For bulk systems, theory predicts that the scaling behavior of the RFIM depends on $H_0^2|t|^{-\phi}$ where H_0 is the random-field intensity, $t=[T-T_c(H_0)]/T_c(H_0)$ is a reduced temperature [2,8,19–21], and [19] the crossover exponent is $\phi=\gamma$, the pure Ising susceptibility exponent. For $d>2$, $T_c(H_0)$ is the field-dependent temperature at which a sharp transition still occurs; in $d=2$ the dominant terms still depend on the same combination, where now [21] "$T_c(H_0)$" denotes a pseudocritical temperature marking, e.g., the location of the rounded specific-heat peak. In $d=2$, specific heat [20] and neutron-scattering [21] data are in good agreement both with the choice of scaling variable as above, and with the exactly known $\gamma=7/4$. For the excess free energy $\Delta' f \equiv f(t,H_0) - f(t,0)$ in two dimensions, an additive logarithmic correction arises [20,27]:

$$\Delta' f = A^* t^2 \ln H_0 + H_0^{2d\nu/\phi} \Psi(t\, H_0^{-2/\phi}). \tag{29}$$

In Ref. [9], we showed that the appropriate FSS variable for the description of correlation functions in finite RF systems at $t=0$ is $x \equiv L\, H_0^{2\nu/\phi}$. While the second term on the right hand side of Eq. (29) is taken care of in that way, the logarithm needs separate consideration. On the basis of renormalization-group arguments, in which L^{-1} is seen as an additional relevant field [28], one realizes that the steps leading to the appearance of the $t^2 \ln H_0$ term in Eq. (29) also apply here. Indeed, since the respective eigenvalue [$y_T=1$ in that case, $y_{L^{-1}}=1$ here] divides the dimensionality $d=2$ [20,27]), a corresponding scenario obtains at $t=0$ and $L^{-1} \to 0$, when $L^{-1/\nu}$ is substituted for t. Therefore, we assume

$$\Delta' f(t=0,L,H_0) = \tilde{A} L^{-2} \ln H_0 + H_0^{2d\nu/\phi} \tilde{\Psi}(L\, H_0^{2\nu/\phi}). \tag{30}$$

In Fig. 8, where $T=T_{c\ 0}$ (thus a small, H_0-dependent shift in "$T_c(H_0)$" [20,21] has been neglected, which should not matter much for low RF intensities), we display results of a numerical test of Eq. (30), both with and without the logarithmic term.

We have found fits of a quality similar to that shown in Fig. 8(b), where $\tilde{A}=10^{-4}$, for a wide range $10^{-5} \lesssim \tilde{A} \lesssim 10^{-2}$ along which the χ^2 estimator remains approximately constant. At large $H_0 L^{\phi/2\nu}$, however, the fits deteriorate noticeably [not obvious from Fig. 8(b), because of the large vertical scale], no doubt owing to the incipient breakdown of the small-RF regime [where, e.g., the H_0-dependent shift in "$T_c(H_0)$" is no longer negligible]. Comparison with experimental data, e.g., from Ref. [20] is not straightforward, as transforming from bulk scaling, [Eq. (29)] to FSS [Eq. (30)] may involve numerical factors not immediately available.

Moving on toward incorporating both RF and uniform field effects, we again neglect the H_0-dependent shift in

''$T_c(H_0)$,'' and make $T=T_{c\,0}$. In the presence of several relevant fields $u_1, u_2 \ldots$ with respective scaling powers $y_1, y_2, \ldots$, the singular part of the free energy scales as [27]

$$f(u_1,u_2,\cdots)=|u_1|^{d/y_1}F\left(\frac{u_2}{|u_1|^{y_2/y_1}},\frac{u_3}{|u_1|^{y_3/y_1}},\cdots\right). \tag{31}$$

Using $u_1=H_0$, $u_2=L^{-1}$, $u_3=h$, in the case one has ($d=2$): $y_1=2\nu/\phi=8/7$, $y_2=1$, $y_3=y_h=15/8$, therefore

$$f(H_0,L,h)=H_0^{2d\nu/\phi}F(L\,H_0^{2\nu/\phi},h\,H_0^{-2\nu y_h/\phi}). \tag{32}$$

Possible $\ln H_0$ corrections in the manner of Eq. (30) have been omitted, since our interest will focus on the calculation of the Gibbs free energy, which in the case depends on $\Delta'' f=f(H_0,L,h)-f(H_0,L,h=0)$ [see Eqs. (21)–(25)]; we are thus assuming that, at least for small enough h, the logarithmic terms cancel in the subtraction.

Similarly to the pure case but always at $t=0$ and $L^{-1}\to 0$, we investigate the small-h regime, in which one expects $\Delta'' f=a(L,H_0)\,h^{\mu}$. From Eq. (32), this implies

$$\Delta'' f=h^{\mu}\,H_0^{2\nu(d-\mu y_h)/\phi}F_1(L\,H_0^{2\nu/\phi}). \tag{33}$$

By assuming, as $H_0\to 0$, a power-law dependence $F_1(x)\sim x^t$, and demanding that, in this limit, (i) the H_0-dependence of $\Delta'' f$ must vanish and (ii) the form $h^2 L^{\gamma/\nu}$ be reobtained, one obtains $\mu=2$, $t=7/4$. Therefore, for small $h\lesssim L^{-y_h}$ one generally has

$$\Delta'' f=\left(\frac{h}{H_0}\right)^2 F_1(L\,H_0^{2\nu/\phi}). \tag{34}$$

Now considering a nonvanishing, but still small RF, one may assume a crossover to a new power-law form for $F_1(x)$, $F_1(x)\sim x^z$. In this regime ($L\,H_0^{2\nu/\phi}\gtrsim 1$),

$$\Delta'' f=L^z\,H_0^{2\nu z/\phi-2}h^2; \tag{35}$$

thus $a(L,H_0)=L^z\,H_0^{2\nu z/\phi-2}$, yielding (see Sec. VI A)

$$g(L,H_0,m)=-[a(L,H_0)]^{-1}m^2=-L^{-z}H_0^{2-2\nu z/\phi}m^2. \tag{36}$$

Our data for $g(L,H_0,m)$, displayed in Fig. 9, are consistent with $z=1$, that is, $g(L,H_0,m)\sim -L^{-1}\,H_0^{6/7}\,m^2$.

One then has, using Eq. (26),

$$P_0(M)=\exp[-g_1 L_x H_0^{6/7}m^2], \tag{37}$$

with $g_1\simeq 0.28$ from the slope of the straight line in Fig. 9. Therefore, the distribution is still Gaussian, with a width $\mathcal{W}\sim g_1^{-1/2}H_0^{-3/7}/\sqrt{L_x}$. A comparison with a corresponding pure system [see Eq. (28) and the arguments in the paragraph preceding it] gives

$$\frac{\mathcal{W}(L,L_x,H_0)}{\mathcal{W}(L,L_x,0)}\sim(L\,H_0^{8/7})^{-3/8}, \tag{38}$$

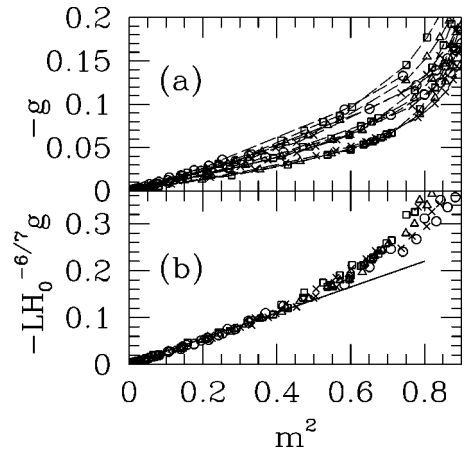

FIG. 9. Negative Gibbs free energies: (a) raw data and (b) scaled, against squared uniform magnetization. Linear scales are used on axes, in order to underline the spread of raw data. In (a), data for the same (L,H_0) are joined by dashed lines. Strip widths: $L=4$ (circles), 6 (crosses), 8 (triangles), and 10 (squares). RF intensities: $H_0=0.3$, 0.4, and 0.5 ($L=4$); for $L=6$, 8, and 10, $H_0=0.2$, 0.3, and 0.4. For fixed L, H_0 increases from bottom to top curves. In (b), plots of $-L\,H_0^{-6/7}\,g$ collapse well onto a straight line against m^2 [Eq. (36) with $z=1$] up to $m^2\simeq 0.4$. The straight line in (b) is a guide to the eye, and has a slope 0.275.

showing again that the FSS variable $x\equiv L\,H_0^{2\nu/\phi}$ is the relevant one. For $x\gg 1$ where RFIM behavior sets in, one sees that distribution widths are smaller for RFIM than in zero field. This is in correspondence with very recent ground-state results [29], where it is found that percolation of, say, upward-pointing spins is made less likely by increasing the random field.

VII. CONCLUSIONS

We have used TM methods to calculate spin-spin correlation functions, Helmholtz free energies, and magnetizations on long strips of width $L=3-18$ sites of the two-dimensional RFIM, close to the zero-field bulk critical temperature.

Through an analysis of the probability distributions of correlation functions for varying spin-spin distances R, we have shown that fits to exponential decay of averaged values against R (for R not too large) give rise to effective correlation lengths *larger* than in zero field. This is because of the reinforcement of correlations within domains. At longer distances (i.e., across many domain walls, $R/L\gg 1$), fits of exponential decay become unreliable, thus compromising definitions of effective correlation lengths.

We have worked out explicit connections between field and correlation function distributions at high temperatures, yielding approximate analytical expressions for the latter. Such expressions account well for trends found in numerical data, namely, the existence of peaked cusps and the functional dependence, on R and field intensity H_0, of data below the peak; above the peak, although agreement with numerics is not good, we have pinpointed that the responsibilty for this lies in a truncation in our approximate scaling scheme, which

decouples scaled nearest-neighbor interactions from the random field. We have discussed the use of analytical expressions, such as the ones found here, for a computation of the corresponding structure factor. Though results as they stand are far from conclusive, we have established a rough guide to attempts at connecting basic microscopic features, such as fluctuations of accumulated fields, to experimentally observable quantities, e.g. scattering functions.

We have reanalyzed the asymptotic behavior of the relative widths of correlation function distributions, first presented in Ref. [9], and now complemented by additional data. While our earlier analysis seemed to point towards exponential saturation, the new set of data shows that, for fixed $R/L=1$, the fractional widths of correlation function distributions behave consistently with asymptotic power-law saturation, i.e., depending on $L^{-2.2}$, see Eq. (20). The scaling variables remain as given previously.

Considering a uniform applied field h, we have derived a connection between Helmholtz free energy $f(h)$, uniform magnetization $m(h)$, the Gibbs free energy $g(m)$, and the distribution function for the uniform magnetization in zero uniform field, $P_0(m)$, which is in principle applicable to any finite system. By working at the bulk zero-field critical temperature $T_{c\ 0}$, we have illustrated our approach by showing that, for strips, one indeed obtains a Gaussian distribution [16,18] for m not very close to saturation. Near $m=1$, where scaling breaks down and a single-spin-flip picture holds, a perturbation expansion accounts for the properties of $g(m)$. Still at $T_{c\ 0}$, now in nonzero random field, we have found from finite-size scaling and crossover arguments, coupled with numerical data, that for strip geometries $P_0(m)$ is still Gaussian, and its width varies against (non-vanishing, but small) random-field intensity H_0 as $H_0^{-3/7}$. This is again valid far from saturation (typically, for $m^2 \lesssim 0.4$; see Fig. 9). The ratio between the width of $P_0(m)$ and the width of the corresponding distribution for a strip of same length and width in zero field varies as $(L\,H_0^{8/7})^{-3/8}$.

We expect that at least some of the features discussed here, for distributions of correlation functions and magnetizations on strips, translate also for other geometries. Considering, for instance, square systems: does the nontrivial form of $P_0(m)$ at bulk criticality in zero field [16–18] evolve into a corresponding shape for $H_0 \neq 0$ which depends on the variable $(L\,H_0^{8/7})^{-3/8}$ as here? Finally, recalling possible connections with experiment: given that the description of correlation decay via effective correlation lengths runs into difficulties at long distances, perhaps this compromises naive fits of neutron-scattering data in the small-wave vector region.

In practical terms, the most direct implication of this is that data for this region is most subject to fluctuations. Therefore, if one considers statistical errors of data, they are expected to be larger near zero wave vector. Use of standard data-weighting techniques [30] should contribute toward reducing the overall effects of such fluctuations. Recall that what we have given is the sample-averaged scattering function $[S(q)]$ measured in experiment; though from Eqs. (2) and (3) one might conceivably work out the probability distribution of $S(q)$, the experimentally observable quantity is of considerably greater interest. Another suggestion would be cutting off the data collection below an optimum wave vector dependent on the random field; or, since detectors are designed for a particular range of wave vectors, one might suggest appropriately limiting the range of field values for a given range of q's.

ACKNOWLEDGMENTS

S.L.A.d.Q. thanks the Department of Theoretical Physics at Oxford, where this work was initiated, for the hospitality, and the cooperation agreement between CNPq and the Royal Society for funding his visit. The research of S.L.A.d.Q. was partially supported by the Brazilian agencies CNPq (Grant No. 30.1692/81.5), FAPERJ (Grants Nos. E26–171.447/97 and E26–151.869/2000) and FUJB-UFRJ. R.B.S. acknowledges partial support from EPSRC Oxford Condensed Matter Theory Rolling Grant GR/K97783.

[1] Y. Imry and S. Ma, Phys. Rev. Lett. **35**, 1399 (1975).
[2] S. Fishman and A. Aharony, J. Phys. C **12**, L729 (1979).
[3] H. Yoshizawa, R. A. Cowley, G. Shirana, R. J. Birgeneau, H. J. Guggenheim, and H. Ikeda, Phys. Rev. Lett. **48**, 438 (1982).
[4] R. J. Birgeneau, H. Yoshizawa, R. A. Cowley, G. Shirane, and H. Ikeda, Phys. Rev. B **28**, 1438 (1983).
[5] D. P. Belanger, A. R. King, V. Jaccarino, and J. L. Cardy, Phys. Rev. B **28**, 2522 (1983).
[6] J. Z. Imbrie, Phys. Rev. Lett. **53**, 1747 (1984); J. Bricmont and A. Kupiainen, *ibid.* **59**, 1829 (1987); M. Aizenman and J. Wehr, *ibid.* **62**, 2503 (1989).
[7] For a review, see, e.g., D. P. Belanger, in *Spin Glasses and Random Fields*, edited by A. P. Young (World Scientific, Singapore, 1998).
[8] A. Aharony and E. Pytte, Phys. Rev. B **27**, 5872 (1983).
[9] S. L. A. de Queiroz and R. B. Stinchcombe, Phys. Rev. E **60**, 5191 (1999).
[10] T. Olson and A. P. Young, Phys. Rev. B **60**, 3428 (1999).
[11] C. Chatelain and B. Berche, Nucl. Phys. B **572**, 626 (2000).
[12] M. F. Collins, *Magnetic Critical Scattering* (Oxford University, Oxford, 1989).
[13] Z. Slanic, D. P. Belanger, and J. A. Fernandez-Baca, Phys. Rev. Lett. **82**, 426 (1999); e-print cond-mat/0012343.
[14] U. Glaus, Phys. Rev. B **34**, 3203 (1986).
[15] T. W. Burkhardt and B. Derrida, Phys. Rev. B **32**, 7273 (1985).
[16] G. Kameniarz and H. W. J. Blöte, J. Phys. A **26**, 201 (1993).
[17] K. Binder, Z. Phys. B: Condens. Matter **43**, 119 (1981); D. Nicolaides and A. D. Bruce, J. Phys. A **21**, 233 (1988); R. Hilfer and N. B. Wilding, J. Phys. A **28**, L281 (1995); M. M. Tsypin and H. W. J. Blöte, Phys. Rev. E **62**, 73 (2000).
[18] Y. Tomita, Y. Okabe, and C.-K. Hu, Phys. Rev. E **60**, 2716 (1999); Y. Okabe, K. Kaneda, Y. Tomita, M. Kikuchi, and C. K. Hu, Physica A **281**, 233 (2000).
[19] A. Aharony, Phys. Rev. B **18**, 3318 (1978).

[20] I. B. Ferreira, A. R. King, V. Jaccarino, J. L. Cardy, and H. J. Guggenheim, Phys. Rev. B **28**, 5192 (1983).

[21] V. Jaccarino, A. R. King, and D. P. Belanger, J. Appl. Phys. **57**, 3291 (1985); D. P. Belanger, S. M. Rezende, A. R. King, and V. Jaccarino, *ibid.* **57**, 3294 (1985); A. R. King, V. Jaccarino, M. Motokawa, K. Sugiyama, and M. Date, *ibid.* **57**, 3297 (1985).

[22] M. N. Barber, in *Phase Transitions and Critical Phenomena*, edited by C. Domb and J. L. Lebowitz (Academic, New York, 1983), Vol. 8.

[23] H. W. J. Blöte and M. P. Nightingale, Physica A **112**, 405 (1982).

[24] H. Saleur and B. Derrida, J. Phys. (France) **46**, 1043 (1985).

[25] B. Derrida, B. W. Southern, and D. Stauffer, J. Phys. (France) **48**, 335 (1987).

[26] R. B. Stinchcombe, G. Horwitz, R. Brout, and F. Englert, Phys. Rev. **130**, 155 (1963).

[27] T. Niemeijer and J. M. J. van Leeuwen, in *Phase Transitions and Critical Phenomena*, edited by C. Domb and M. S. Green (Academic, New York, 1976), Vol. 6.

[28] M. P. Nightingale, in *Finite Size Scaling and Numerical Simulations of Statistical Systems*, edited by V. Privman (World Scientific, Singapore, 1990).

[29] E. T. Seppälä and M. J. Alava, Phys. Rev. E **63**, 066109 (2001).

[30] W. Press, B. Flannery, S. Teukolsky, and W. Vetterling, *Numerical Recipes in Fortran, The Art of Scientific Computing*, 2nd ed. (Cambridge University Press, Cambridge, 1994), Chap. 15.